Ultrasound in Med. & Biol., Vol. 32, No. 4, pp. 483–490, 2006

0301-5629/06/$–see front matter

ELSEVIER

doi:10.1016/j.ultramedbio.2005.12.006

CARDIAC MOTION ANALYSIS FROM ULTRASOUND SEQUENCES USING NONRIGID REGISTRATION: VALIDATION AGAINST DOPPLER TISSUE VELOCITY

M. J. Ledesma-Carbayo,* P. Mahía-Casado,† A. Santos,* E. Pérez-David,† M. A. García-Fernández,† and M. Desco†

*Universidad Politécnica de Madrid; and †Hospital G. Universitario Gregorio Marañón, Madrid, Spain

(*Received* 16 *June* 2005, *revised* 28 *November* 2005, *in final form* 9 *December* 2005)

Abstract—Early detection of cardiac motion abnormalities is one of the main goals of quantitative cardiac image processing. This article presents a new method to compute the 2-D myocardial motion parameters from gray-scale 2-D echocardiographic sequences, making special emphasis on the validation of the proposed technique in comparison with Doppler tissue imaging. Myocardial motion is computed using a frame-to-frame nonrigid registration technique on the whole sequence. The key feature of our method is the use of an analytical representation of the myocardial displacement based on a semilocal parametric model of the deformation using Bsplines. Myocardial motion analysis is performed to obtain displacement, velocity and strain parameters. Robustness and speed are achieved by introducing a multiresolution optimization strategy. To validate the method, velocity measurements in three different regions-of-interest in the septum have been compared with those obtained with Doppler tissue velocity in healthy and pathologic subjects. Regression and Bland-Altman analysis show very good agreement between the two different approaches, with the great advantage that the new method overcomes the angle-dependency limitations of the Doppler techniques, providing both longitudinal and radial measurements. (E-mail: mledesma@die.upm.es)

Key Words: **Cardiac motion, Echocardiography, Tissue Doppler imaging, Nonrigid registration, Myocardial motion.**

INTRODUCTION

Cardiac motion analysis constitutes an important aid for the quantification of the elastic and contractility properties of the myocardium. Localized regions with movement abnormalities are related to the existence of ischemic segments, damaged by insufficient tissue microcirculation (Jamal et al. 2001; Weidemann et al. 2003).

Together with cardio-magnetic resonance imaging (-MRI), bidimensional echocardiography is nowadays the reference modality to study the regional myocardial function in clinical practice. Despite the efforts of the medical imaging community, subjective interpretation of ultrasound sequences is still the method of reference in practice. Inter-institutional studies have reported important disagreements on regional analysis among medical centers (Hoffmann et al. 1996), making explicit the need for quantitative methodologies. Clinical and *in vivo* validations of any new method are the most important steps to provide tools that may have a real impact on the clinical routine.

Address correspondence to: María J. Ledesma-Carbayo, Dept. Ingeniería Electrónica, ETSI Telecomunicación, E-28040 Madrid, Spain. E-mail: mledesma@die.upm.es

Quantitative motion analysis in echocardiography has been mainly addressed using Doppler tissue velocity (DTV) techniques. This approach, however, has a disadvantage: its angle dependency because it only measures the velocity throughout the ultrasound beam direction. Other approaches have explored the possibility of obtaining multi-dimensional motion using speckle tracking (Kaluzynski et al. 2001) and elastographic techniques (Konofagou and Ophir 1998; D'hooge et al. 2002). These methods are based on processing the RF signal to obtain the displacement of one or several consecutive lines of response, using correlation and phase shift techniques (Hein and O'Brien 1993).

Other methods combine image feature extraction with deformable and mechanical models. They have been intensively applied to obtain myocardial motion parameters from tagged MRI (Shi et al. 2000; Declerck et al. 1998) and, recently, from echocardiographic data (Papademetris et al. 2001). The main drawback of these methods is that the computed motion strongly depends on a proper segmentation of the myocardial borders, a very difficult task on ultrasound data due to its poor signal-to-noise ratio. Optical flow techniques are also providing promising results, as shown in recent validations (Sühling et al. 2004; Adam et

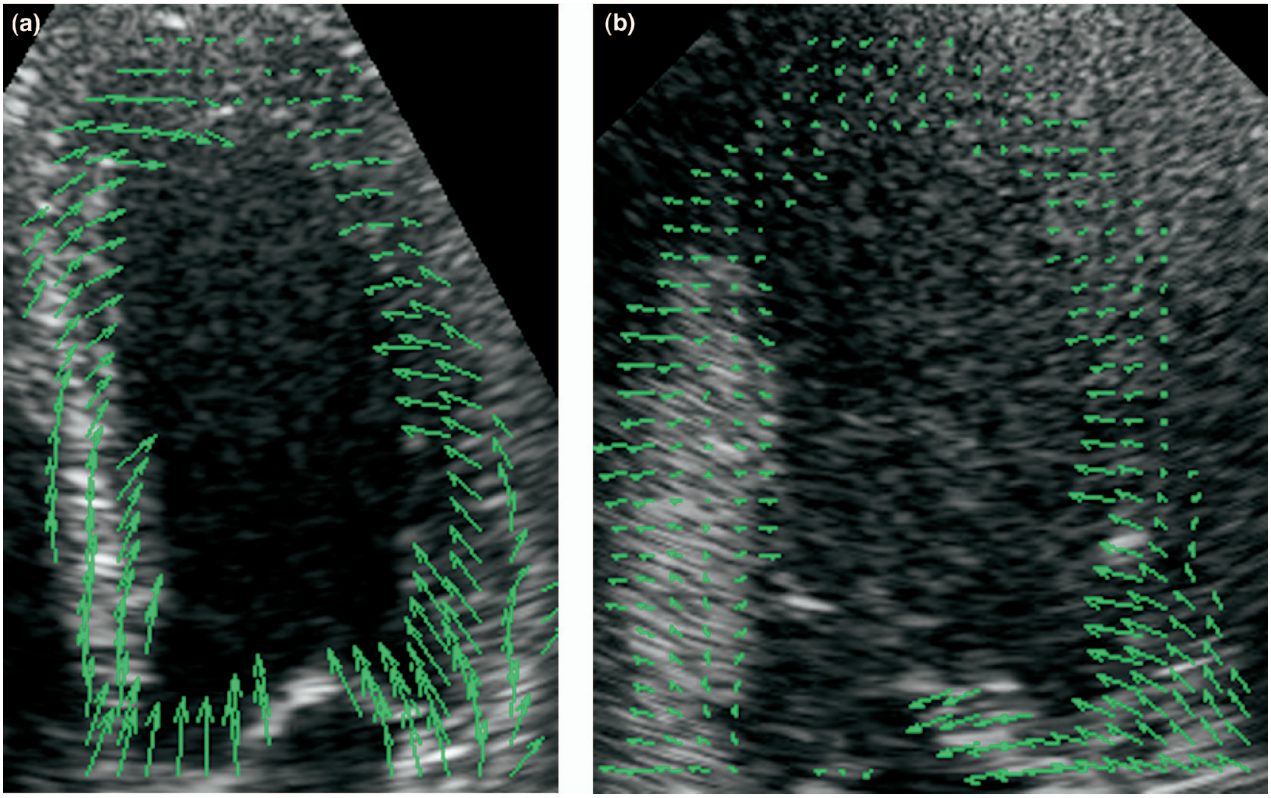

Fig. 1. Displacement field at the end of systole for two different subjects; a healthy subject (a) and a patient with extended akinesia (b).

al. 2004). Sühling et al. (2004) also validate their method comparing their results with DTV.

This paper presents the validation of a new method to analyze the bidimensional myocardial mechanics from gray-scale 2-D echocardiographic sequences applying nonrigid registration techniques. Prior works using nonrigid registration have also been recently applied to tagged MR studies to compute cardiac motion (Chandrashekara et al. 2004). Our work shows the validity of these techniques on gray-level echocardiographic data by comparing the results with DTV measurements.

The article is organized as follows. In the next section, we present the method used to compute the dense myocardial motion field and other derived parameters presented. The following two sections describe the validation methodology and its results, to end with discussion and conclusions in the final section.

MYOCARDIAL MOTION ANALYSIS USING NONRIGID REGISTRATION

Dense displacement field computation

Given an image sequence $f(t, \mathbf{x})$, the goal is to estimate a dense displacement field $\mathbf{g}(t, \mathbf{x})$ over the whole sequence. We choose to represent the movement with respect to the first frame of the sequence: a point at coordinate $\mathbf{x}$ in the first frame ($t = t_0$) will move to the location $\mathbf{g}(t, \mathbf{x})$ at time t. Formulation is therefore defined as:

$$\mathbf{g}(t, \mathbf{x}) \equiv \mathbf{g}_t(\mathbf{x}) \text{ where } t \in \{0,\ 1,\ \ldots,\ T-1\} \text{ and } \mathbf{x} \equiv (x_1,\ x_2) \equiv \mathbf{I} \quad (1)$$

where $\mathbf{I}$ is the set of coordinates that specify the spatial region-of-interest (ROI) and t is the temporal axis in frames (T being the total number of frames). We express $\mathbf{g}(t, \mathbf{x})$ as a series of transformations between consecutive pairs of images $\mathbf{g}'_t(\mathbf{x}_{t-1})$ found through independent nonrigid registration processes.

$$\mathbf{g}_t(\mathbf{x}) = \mathbf{g}'_t(\mathbf{x}_{t-1}) + \mathbf{g}_{t-1}(\mathbf{x}) \text{ where } \mathbf{x}_{t-1} = \mathbf{g}_{t-1}(\mathbf{x}) \text{ and } \mathbf{g}_0(\mathbf{x}) = \mathbf{x} \quad (2)$$

The transformation between consecutive frames $\mathbf{g}'_t$ is defined as a linear combination of Bspline basis functions, located in a rectangular grid, as previously introduced in Kybic and Unser (2003) and Ledesma-Carbayo et al. (2001):

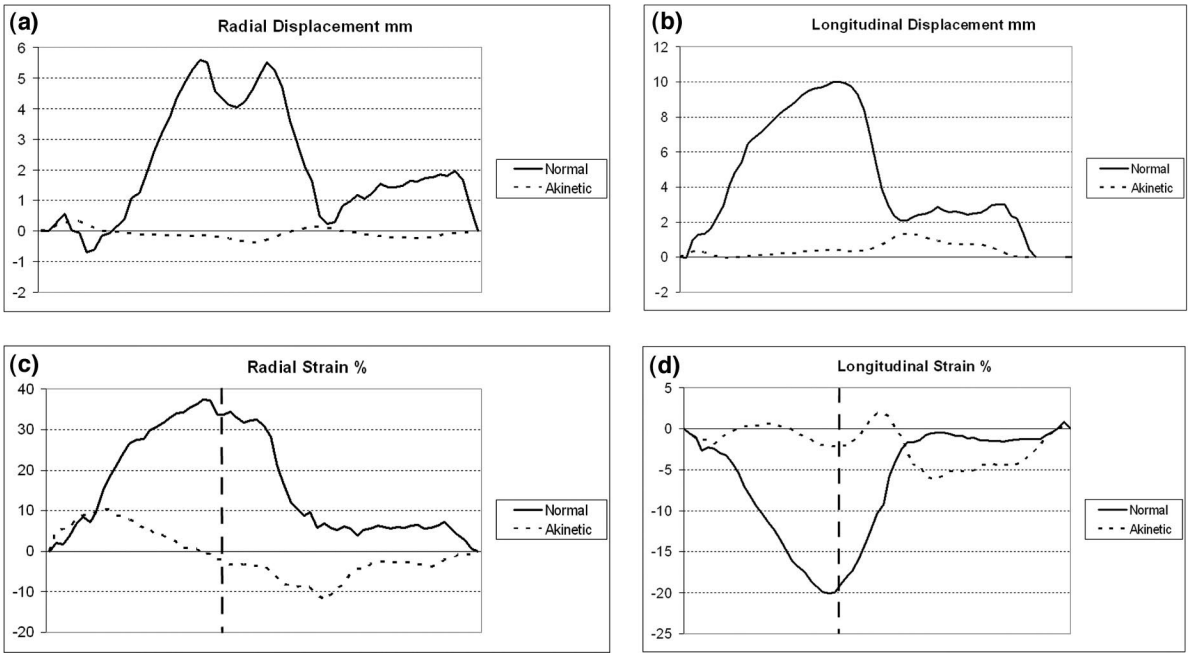

Fig. 2. (a, c) Radial and (b, d) longitudinal displacement and strain time curves of the medial septal segment for a normal and an akinetic segment from two different subjects. End of systole is marked with a vertical dashed line. The x-axis represents time normalized to the cardiac cycle.

$$\mathbf{g}'_t(\mathbf{x}) = \sum_{\mathbf{j}\in Z^N} \mathbf{c}_\mathbf{j}\beta_r(\mathbf{x})/h - \mathbf{j} \tag{3}$$

The scale parameter h determines the space between the grid knots and, therefore, the number of parameters $\mathbf{c_j}$ and the smoothness of the solution. The solution to this problem is formulated as an optimization procedure that minimizes a criterion E to find the coefficients $\mathbf{c_j}$. E is defined as the sum of squared differences between consecutive frames. This optimization is solved by using a gradient descent method. We generate a continuous version of the discrete image $f(t, \mathbf{x})$ at $(t = t')$ by spline interpolation; providing an excellent framework to find a subpixel solution and to compute the spatial derivatives analytically and, therefore, the gradient. Speed and robustness are guaranteed using a multiresolution approach both in the image and transformation space, creating a pyramid optimal in the L_2-sense taking advantage of the spline representation (Unser et al. 1993).

The displacement field is also constrained using *a priori* knowledge about the cardiac motion field. Firstly, the motion at the reference frame $f(0, \mathbf{x})$ must be zero and, secondly, we impose the cyclic behavior as $\mathbf{g}(0, \mathbf{x}) = \mathbf{g}(T, \mathbf{x})$. This last constraint is achieved by performing the registration process in both directions (forward and backward), obtaining two estimations of the displacement at a given time t. The final estimation is computed as a weighted linear combination of both estimates, which is the maximum likelihood (ML) estimate of the motion field considering the error distribution of the registration as independent, identically distributed and normal.

$$\mathbf{g}_t(\mathbf{x}) = \omega_t \mathbf{g}_t^f(\mathbf{x}) + (1-\omega_t)\mathbf{g}_t^b(\mathbf{x}) \text{ with } \omega_t = \frac{(T-t)}{T} \tag{4}$$

For the particular application in conventional echocardiography presented in this paper, we used quadratic Bsplines to represent the deformation and we chose a scale parameter h in pixels equivalent to 1 cm. The optimum values for both the degree of Bsplines and the parameter h were obtained through validation on synthetic sequences, as described in Ledesma-Carbayo (2003).

Spatiotemporal derived parameters

Once the displacement field is obtained, other parameters of clinical interest are computed. Velocity field can be calculated taking into account the time interval between frames.

$$\mathbf{v}(t, \mathbf{x}) = \frac{d\mathbf{g}(t, \mathbf{x})}{dt}. \tag{5}$$

Strain and strain rate are also parameters of great interest, as they provide information about the active contraction of the myocardial segments (D'hooge et al. 2000; Papademetris et al. 2001). Strain is computed

according to continuum mechanics theory (Spencer 1980) following the Green-Lagrange strain tensor. This calculation is computed analytically as we have defined our deformation model continuously through Bspline functions (equation [3]). We obtain the strain rate tensor as a temporal derivative of the strain tensor.

Displacement, velocity, strain and strain rate parameters are usually assessed using their mean values in ROI in the different segments of the myocardium. Radial, longitudinal, and circumferential components are also obtained by projecting the different parameters onto the left ventricular main axis.

This methodology has been tested previously in clinical trials, providing results consistent with published data obtained from tagged MRI (Ledesma-Carbayo et al. 2005; Ledesma-Carbayo 2003). Significant differences were found between normal and pathological segments. As an example, in Figure 1, we show the dense displacement field obtained from a four-chamber view, for a healthy volunteer (left) and a patient with extended akinesia due to an anterior infarct (right).

Figure 2 shows the time evolution of the radial and longitudinal displacement and strain in the medial septal segment for both subjects. The different behavior of the normal and akinetic segments in displacement and strain is clearly noticeable.

VALIDATION

To validate the proposed methodology and the accuracy of the results obtained, the calculated dense velocity field was compared with DTV measurements in 16 healthy and pathologic subjects. Simultaneous acquisition of second harmonic DTV sequences and gray-scale sequences allow the comparison of the two measurements on a pixel-by-pixel basis.

Data acquisition

Second harmonic DTV and conventional gray-scale sequences of the septum were simultaneously acquired from a four-chamber apical view in 16 different subjects. The subjects were chosen to show different velocity values and temporal patterns. Eight healthy volunteers (N_i) and eight patients (P_i) with abnormal myocardial contractility (five of them with left bundle branch block and three with dilated myocardiopathy) were studied. A 2.0- to 5.0-MHz transducer was used on a Sequoia C-512 system (Siemens AG, Munich, Germany). The parameters of the scanner were set to obtain a good frame rate and a good velocity dynamic range, avoiding aliasing while having a good Doppler velocity representation. Frame rate varied from 80 to 120 fps, and maximum Doppler velocity span was normally set to 12.03 cm/s. The RGB Doppler codification look-up table (LUT) was chosen to be linear with respect to velocity. Among the LUTs provided by the scanner, *V*.1 provided the best linear behavior in the whole velocity span (Desco et al. 2002). The field-of-view was adjusted to cover the whole septum, without giving priority to the alignment of the septum to the ultrasound beam. Images were digitally stored in a cine-loop format (multiframe DICOM 3.0 standard) for subsequent off-line analysis. All the sequences covered a complete cardiac cycle determined both by the ECG and the phonocardiogram signal.

Statistical analysis

DTV sequences were processed to obtain a Doppler velocity estimation (v_D) throughout the whole cycle and for every point in the septum. RGB values for every point and time frame were decoded using the codification LUT *V*.1 (Desco et al. 2002). The maximum velocity span value was extracted from the DICOM header for every sequence.

The dense velocity field was calculated following the procedure described earlier. The velocity vector for every point and every time frame was calculated as the incremental displacement between two consecutive frames divided by the time interval $\left(\mathbf{v}_{2D} = \frac{\mathbf{g}'_i(\mathbf{x})}{\Delta t}\right)$. Δt was extracted from the DICOM header. The bidimensional vector $\mathbf{v}_{2D}$ was then projected to obtain the component equivalent to the Doppler measurement for every point and time in the sequence. As the Doppler measurement provides the velocity v_D along the ultrasound beam, we needed to compute the beam direction for every point and to project onto this direction the bidimensional velocity vector to obtain an equivalent estimation v_r with our method.

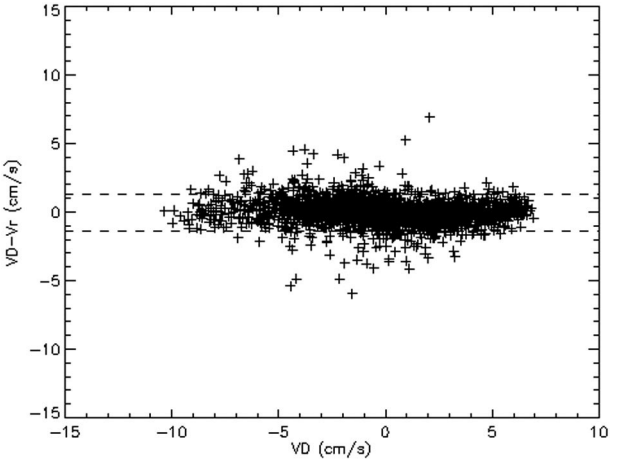

Fig. 3. Bland-Altman plot representing the difference $v_D - v_r$ with respect to the DTV value v_D. Dashed lines correspond to the limits of agreement (mean ± 2 SD). Measurements from all the subjects and ROI are included in the analysis.

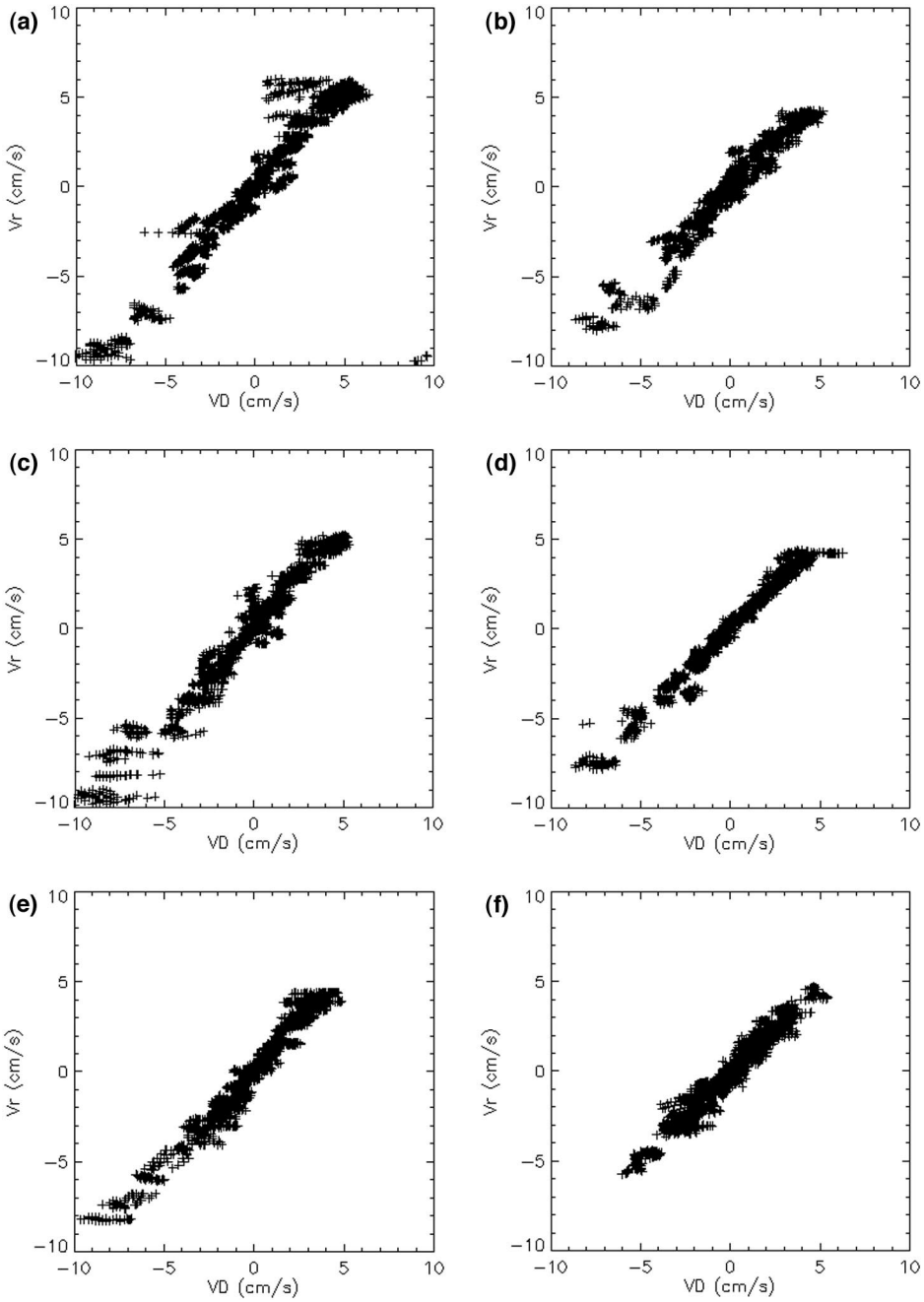

Fig. 4. Scatter plots (v_r with respect v_D) for the three ROIs (basal (a, b), medial (c, d), and apical (e, f)) and two different subjects (N_3 (a, c, e) and P_8 (b, d, f)).

Both velocity estimations v_D and v_r were compared on a pixel-by-pixel basis and throughout the whole cardiac cycle. The comparison consisted in performing linear regression and Bland-Altman analysis in three different regions of the septum. ROI were located in the apical, medial and basal segments of the septum and were carefully placed to avoid Doppler artifacts (Santos et al. 2001), such as black spots, aliasing, or erroneous data at myocardial edges. Typical ROI size was 0.5 cm^2, comprising approximately 10,000 comparisons for each ROI and every subject.

A linear model $v_r = b * v_D + c$ was applied to every ROI and all the frames in the cardiac cycle and assessed by means of regression analysis. The correlation coefficient (R) was computed. Linear regression results were further studied with single-factor analysis of variance to explore statistical dependency on different factors: these

factors were the location of the ROI in the septum and pathologic *vs.* healthy subjects.

A Bland-Altman statistical analysis was also performed to assess the bias between both measurement techniques and their difference dependency on the magnitude of the value v_D.

The linear model was qualitatively shown by means of scatter maps of v_r with respect v_D. Temporal behavior was also assessed qualitatively by displaying the Bland-Altman plot with respect to the temporal coordinate and time evolution curves of the ROI mean values.

RESULTS

Regression analysis

The linear regression analysis was significant ($p < 0.001$) for all the sequences and ROIs analyzed. Table 1 summarizes the regression analysis results for the three septal ROIs in healthy and pathologic subjects. The regression lines were all very close to the line of equality, showing a good agreement between the two measurements v_r and v_D. The average value of the correlation coefficient R was 0.96, indicating a strong linear relationship between the two measurements for all the cases. Single factor analysis of variance with respect to location-of-segment and type-of-subject (healthy or pathologic) showed no significant effects at $p < 0.01$.

Bland-Altman analysis was performed taking into account all the measurements from all the subjects and ROI. It showed a negligible bias between the two measurements, showing a mean velocity difference of −0.061 cm/s and a standard deviation of 0.667 cm/s that corresponds to approximately 5% of the measurement range. Figure 3 shows the Bland-Altman plot of the difference $v_D - v_r$ with respect the reference measurements v_D. Dashed lines correspond to the limits of agreement (mean ±2 SD). The differences between both methods seem not to depend on the magnitude of the measurement.

Linear relationship is also confirmed by observing the scatter plots of v_r with respect to v_D, including all the points of comparison. As an example, Figure 4 shows the scatter plots for two different subjects and the three septal ROI.

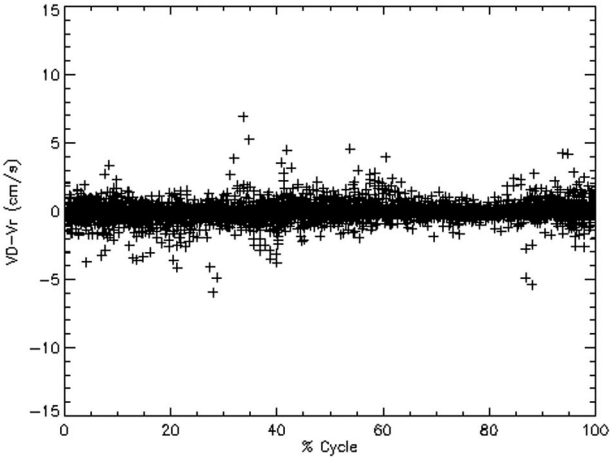

Fig. 5. Bland-Altman plot representing the difference $v_D - v_r$ with respect to a normalized cardiac cycle. Measurements from all the subjects and ROI are included in the analysis.

Temporal dependency

Finally, we checked the agreement of the measurements throughout the cardiac cycle. To show this effect, we studied the dependency of the difference between both methods with respect to a normalized cardiac cycle using a Bland-Altman plot (Fig. 5). The difference is quite small throughout most of the cardiac cycle; however, greater values and more scatter points appear at protosystole and at early and late diastole. These instants of the cardiac cycle are characterized by steep changes and peaks and small temporal shifts may lead to higher differences between both variables.

We also calculated time evolution curves of the mean ROI velocities (Fig. 6). Dashed line represents the Doppler measurement (v_D), and the solid line represents the velocity obtained using nonrigid registration (v_r). We assessed visually the good correspondence throughout the whole cardiac cycle for all the subjects and ROI.

DISCUSSION AND CONCLUSIONS

This work presents the validation of a new method to compute myocardial motion parameters from gray-scale echocardiographic sequences using nonrigid regis-

Table 1. Results of the regression analysis for the eight healthy subjects and the three different ROIs (apical, medial, basal), with the linear model $v_r = b * v_D + c$ (b and c are represented ± their standard error)

	Healthy subjects		Pathological subjects		All cases	
	b	*c*	*b*	*c*	*b*	*c*
Basal	1.02 ± 0.04	0.01 ± 0.10	1.00 ± 0.02	0.01 ± 0.11	1.02 ± 0.04	0.01 ± 0.10
Medial	1.02 ± 0.05	0.12 ± 0.09	0.99 ± 0.02	0.03 ± 0.04	1.01 ± 0.04	0.08 ± 0.08
Apical	1.05 ± 0.05	0.10 ± 0.08	1.04 ± 0.03	0.03 ± 0.07	1.04 ± 0.04	0.07 ± 0.08
All segments	1.03 ± 0.05	0.08 ± 0.10	1.01 ± 0.03	0.03 ± 0.08	1.02 ± 0.04	0.05 ± 0.09

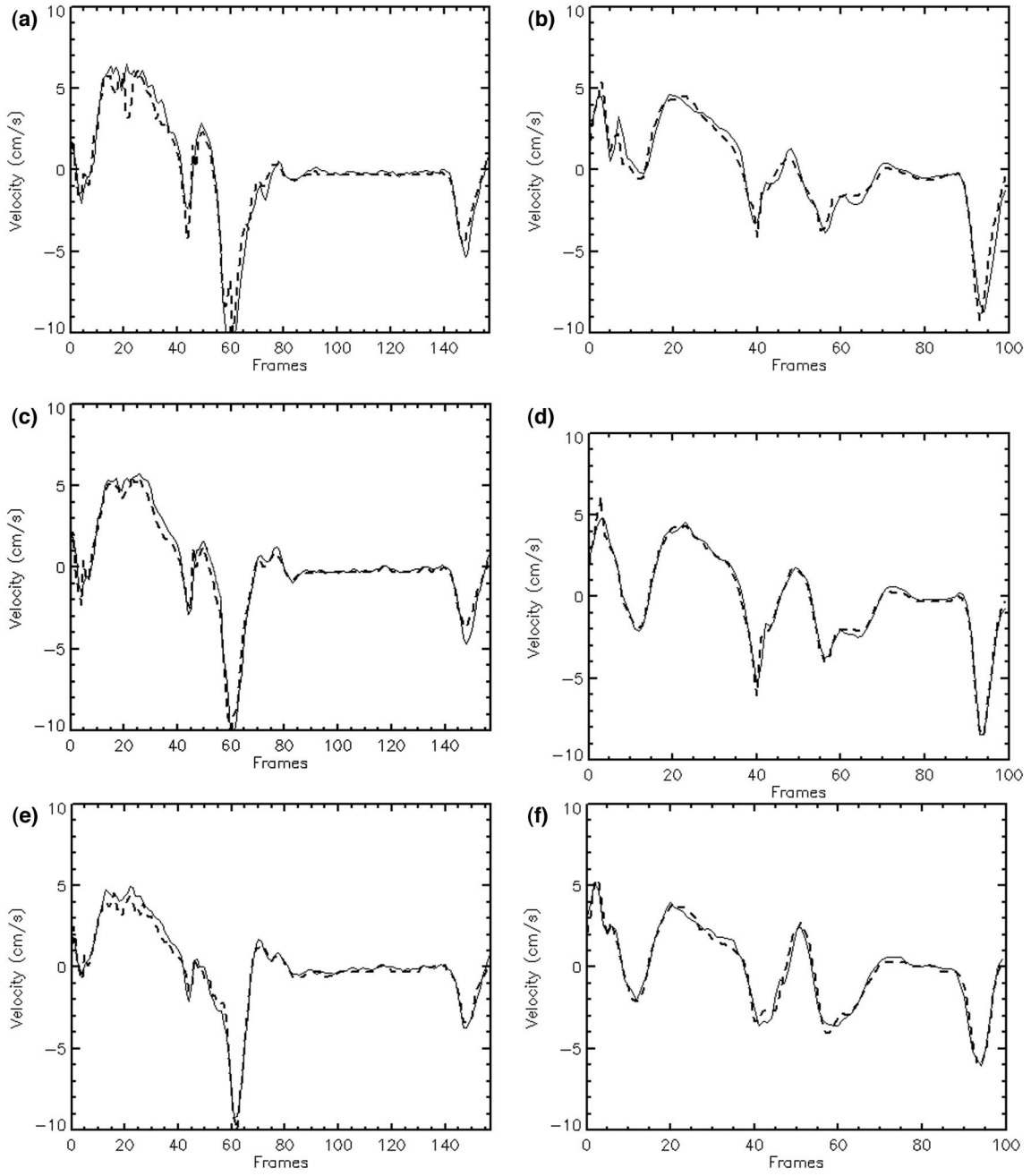

Fig. 6. Time evolution curves of mean ROIs velocities v_r and v_D in two different subjects (N_3 (a, c, e) and P_8 (b, d, f)) and the three septum ROIs studied (basal (a, b), medial (c, d), and apical (e, f)).

tration techniques. Compared with other methods, our approach presents two main advantages: it is angle-independent and it computes the dense myocardial displacement field, as it makes use not only of the myocardial edges but of all the myocardial information. Another important advantage is that myocardial segmentation, a difficult task in echocardiography, is not needed. This methodology can be used to assess cardiac motion in any view and segment, so that motion and deformation can be characterized in 2-D.

Validation has been carried out by comparing with DTV measurements. The experiment has been performed in physiologic conditions in human subjects, covering typical velocity patterns in healthy and pathologic cases. Doppler artifacts have been avoided, to have the best possible measurement of reference.

Results show that there is a linear relationship between computed and acquired measurements, which is, in all the cases, close to the identity. A negligible offset between both measurements was found, confirming that the proposed method may constitute an alternative to the Doppler methods. Sühling et al. (2004) also validated their optical flow method by comparing it with DTV. In comparison with their results in human subjects, we obtained a smaller difference between measurements as well as a regression line closer to the identity. No restrictions have been imposed in the septum orientation with respect to the beam axis; therefore, the velocity measurements validated are a combination of the radial and longitudinal components of the motion, without giving priority to the motion along any particular direction.

Regarding the interpretation of the differences, it should be taken into account that Doppler measurements also suffer from different inaccuracies. Santos et al. (2001) have reported two main sources of error in Doppler velocity imaging: these are a random noise with a standard deviation of 2% of the velocity span and black spots and artifacts at the edges of the myocardium, with much higher inaccuracies (>5%). Walker et al. (2004) have recently reported tissue velocity inaccuracies in the range of 2% to 7% on modern ultrasound systems. The results obtained with our validation showed that the proposed method may have an accuracy similar to that obtained with Doppler methods.

In summary, this work shows the validity of the proposed method to compute myocardial motion, overcoming the angle-dependency limitations of the Doppler methods and providing bidimensional components of the myocardial motion (radial and longitudinal, or radial and circumferential).

Acknowledgements—This work was supported in part by Red Temática IM3 (G03/185) and research projects PI041495 and PI041920, from Spanish Health Ministry.

REFERENCES

Adam D, Landesberg A, Konyukhov E, et al. Ultrasonographic quantification of local cardiac dynamics by tracking real reflectors: Algorithm development and experimental validation. IEEE Comput Cardiol 2004;31:337–340.

Chandrashekara R, Mohiaddin RH, Rueckert D. Analysis of 3d myocardial motion in tagged MR images using nonrigid image registration. IEEE Trans Med Imag 2004;23:1245–1250.

Declerck J, Feldmar J, Ayache N. Defininion of a 4D continuous planispheric transformation for the tracking and the analysis of left-ventricle motion. Med Imag Anal 1998;2:197–213.

Desco M, Ledesma-Carbayo M, Pérez E, et al. Assessment of normal and ischaemic myocardium by quantitative m-mode tissue doppler imaging. Ultrasound Med Biol 2002;28:561–569.

D'hooge J, Heimdal A, Jamal F, et al. Regional strain and strain rate measurements by cardiac ultrasound: Principles, implementation and limitations. Eur J Echocardiography 2000;1:154–170.

D'hooge J, Konofagou E, Jamal F, et al. Two-dimensional ultrasonic strain rate measurement of the human heart in vivo. IEEE Trans Ultrason Ferroelec Fre Qual Control 2002;49:281–286.

Hein I, O'Brien W. Current time-domain methods for assessing tissue motion by analysis from reflected ultrasound echoes—A review. IEEE Trans Ultrason Ferroelec Fre Qual Control 1993;40:84–102.

Hoffmann R, Lethen H, Marwick T, et al. Analysis of interinstitutional observer agreement in interpretation of dobutamine stress echocardiograms. J Am Coll Cardiol 1996;27:330–336.

Jamal F, Strotmann J, Weidemann F, et al. Noninvasive quantification of the contractile reserve of stunned myocardium by ultrasonic strain rate and strain. Circulation 2001;104:1059–1065.

Kaluzynski K, Chen X, Emelianov S, Skovoroda A, O Donnell M. Strain rate imaging using two-dimensional speckle tracking. IEEE Trans Ultrason Ferroelec Fre Qual Control 2001;48:1111–1123.

Konofagou E, Ophir J. A new elastographic method for estimation and imaging of lateral displacements, lateral strains, corrected axial strains and poisson s ratios in tissues. Ultrasound Med Biol 1998; 24:1183–1199.

Kybic J, Unser M. Fast parametric elastic image registration. IEEE Trans Image Process 2003;12:1427–1442.

Ledesma-Carbayo M, Kybic J, Desco M, Santos A, Unser M. Cardiac motion analysis from ultrasound sequences using non-rigid registration. In: Niessen W, Viergever M, eds. MICCAI 2001, Lecture Notes in Computer Science. Springer, 2001, vol. 2208, 889–896.

Ledesma-Carbayo M, Santos A, Mahia P, et al. Longitudinal and radial regional strain obtained from gray-scale conventional echocardiography. J Am Coll Cardiol 2005;45:A255.

Ledesma-Carbayo MJ. Cardiac motion detection using elastic registration. Ph.D. thesis, Universidad Politécnica de Madrid, Spain. 2003.

Papademetris X, Sinusas AJ, Donald DP, Duncan JS. Estimation of 3D left ventricular deformation from echocardiography. Med Image Anal 2001;5:17–28.

Santos A, Ledesma-Carbayo M, Malpica N, et al. Accuracy of heart strain rate calculation derived from doppler tissue velocity data. In: Insana MF, Shug K, eds. Medical imaging 2001. SPIE 2001;4325: 546–556.

Shi P, Sinusas AJ, Constable RT, Ritman E, Duncan JS. Point-tracked quantitative analysis of left ventricular motion from 3D image sequences. IEEE Trans Med Imag 2000;19:36–50.

Spencer AJM. Continuum mechanics. London, United Kingdom: Longman Group, 1980.

Sühling M, Jansen C, Arigovindan M, et al. Multiscale motion mapping: A novel computer vision technique for quantitative, objective echocardiographic motion measurement independent of doppler: First clinical description and validation. Circulation 2004; 110:3093–3099.

Unser M, Aldroubi A, Eden M. The L2-polynomial spline pyramid. IEEE Trans Pattern Anal Mach Intell 1993;15:364–379.

Walker A, Olsson E, Wranne B, Ringqvist I, Ask P. Accuracy of spectral Doppler flow and tissue velocity measurements in ultrasound systems. Ultrasound Med Biol 2004;30:127–132.

Weidemann F, Dommke C, Bijnens B, et al. Defining the transmurality of a chronic myocardial infarction by ultrasonic strain-rate imaging: implications for identifying intramural viability: an experimental study. Circulation 2003;107:883–888.